Supporting information

Figure S1

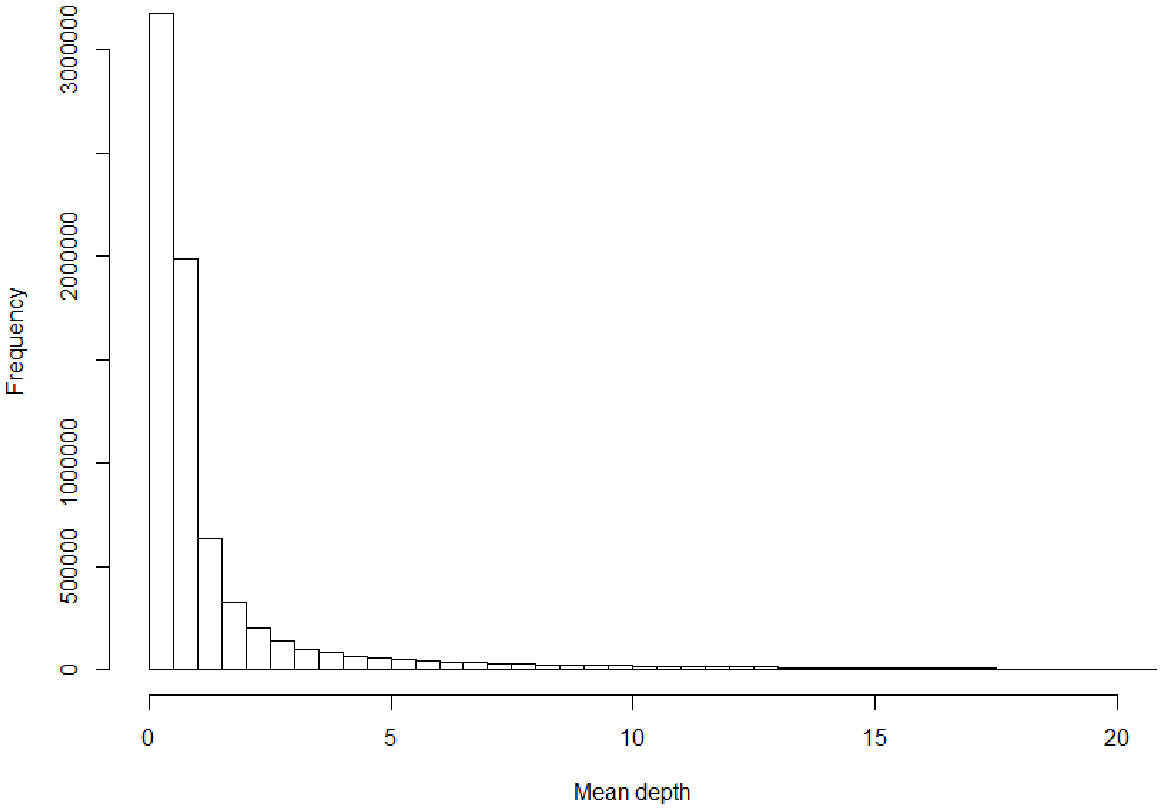

Figure S1. Histogram of the mean depth (number of unique reads) of exome capture sequencing.

Figure S2

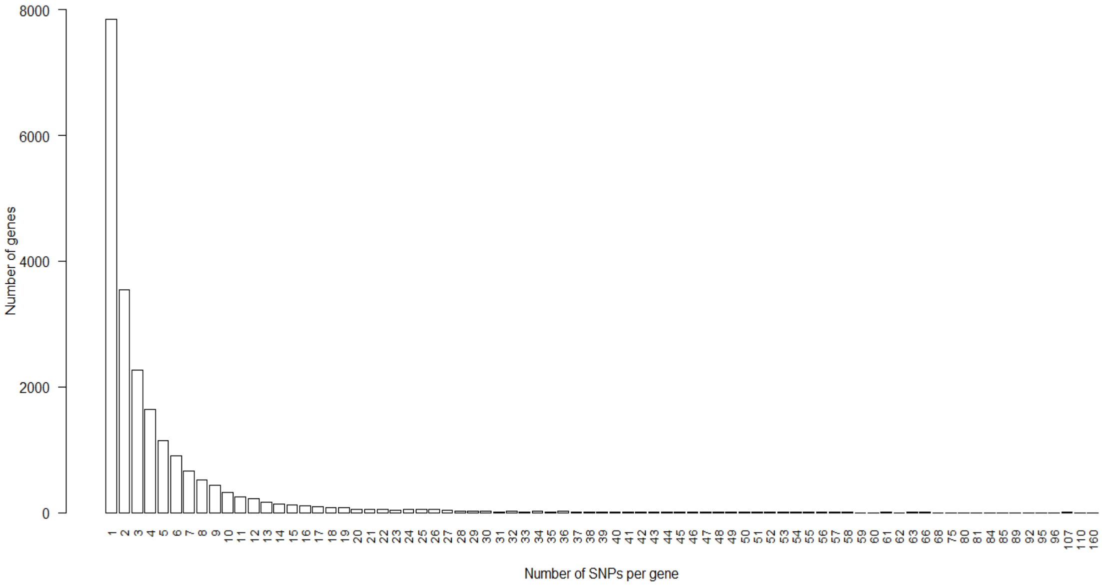

Figure S2. Histogram of the number of single-nucleotide polymorphisms per gene captured by exome sequencing.

Figure S3

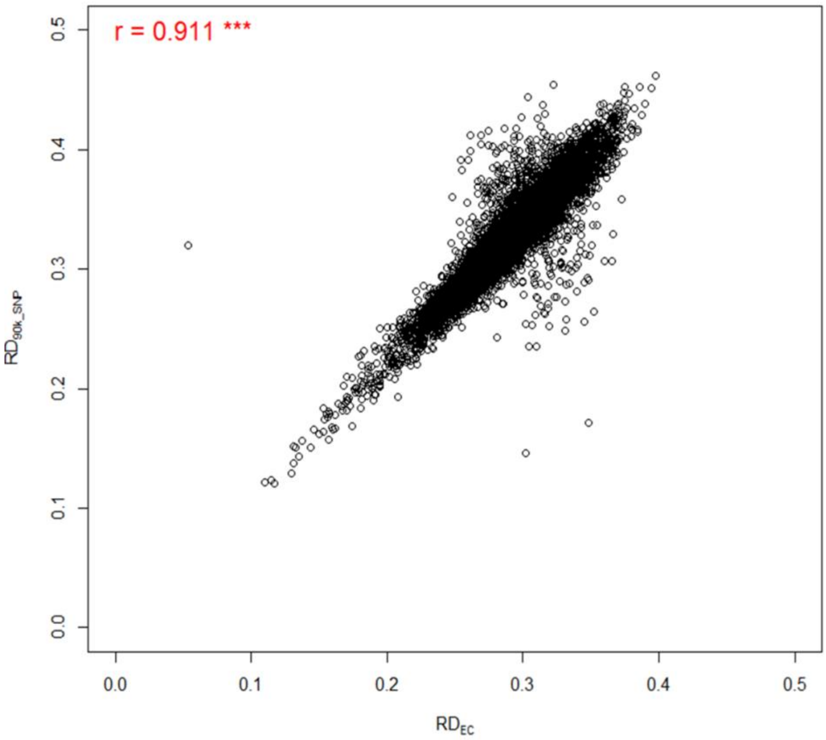

Figure S3. Comparison between Rogers' distances calculated using exome capture sequencing (RD$_{EC}$) and the 90K SNP array data set (RD$_{90K\_SNP}$) for the 133 parents of the population composed by 1,574 wheat hybrids.

The significant (Mantel test: *P-value* < 0.001) Pearson correlation (r) is plotted in the upper-left corner of the plot.

Figure S4

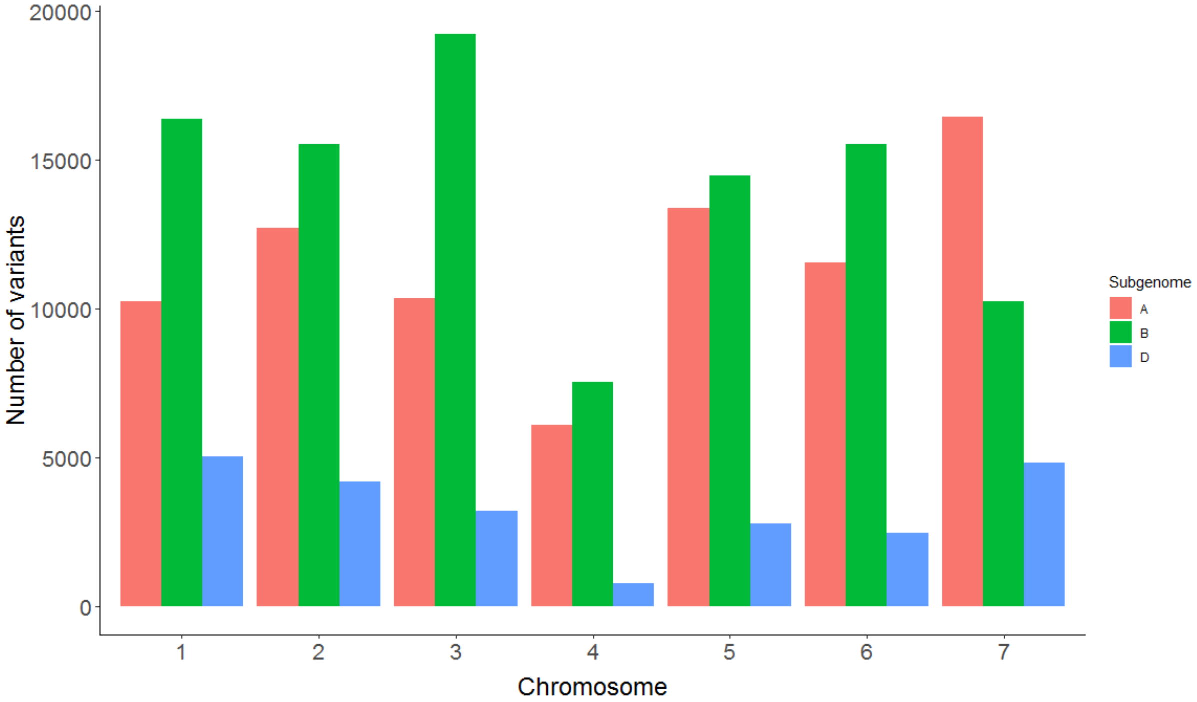

Figure S4. Number of single-nucleotide polymorphisms per wheat chromosome captured by exome sequencing.

Figure S5

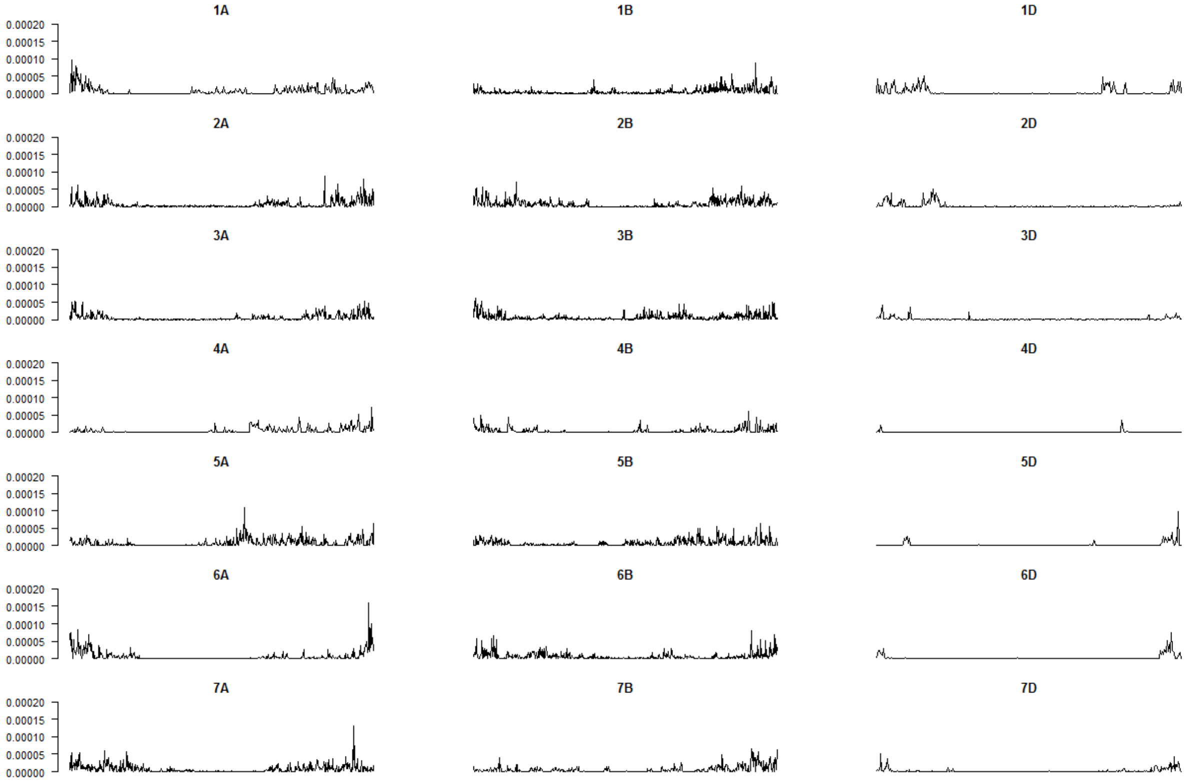

Figure S5. Genome-wide distribution of average exome nucleotide diversity.

Average nucleotide diversity (Pi) was estimated using a sliding window size of 1Mb on the exome capture sequencing data.

Figure S6

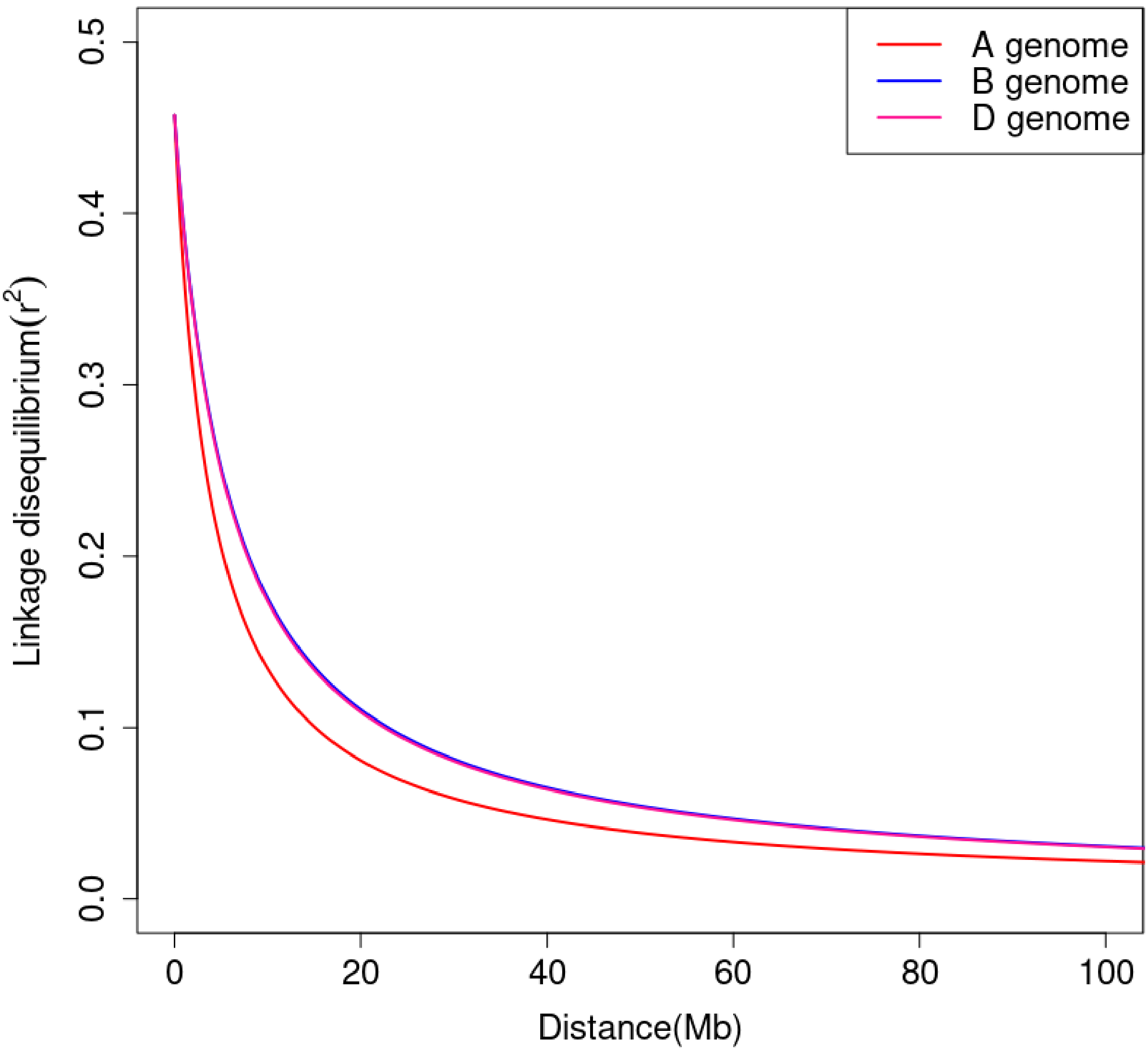

Figure S6. Linkage disequilibrium (r^2) as a function of physical distance (Mb) for the three different wheat subgenomes

In order to make linkage disequilibrium estimates (LD, r^2) comparable across subgenomes, a random sample was taken from marker pairs located within A and B subgenomes considering a sample size equals to the total marker pairs present in the D subgenome.

Figure S7

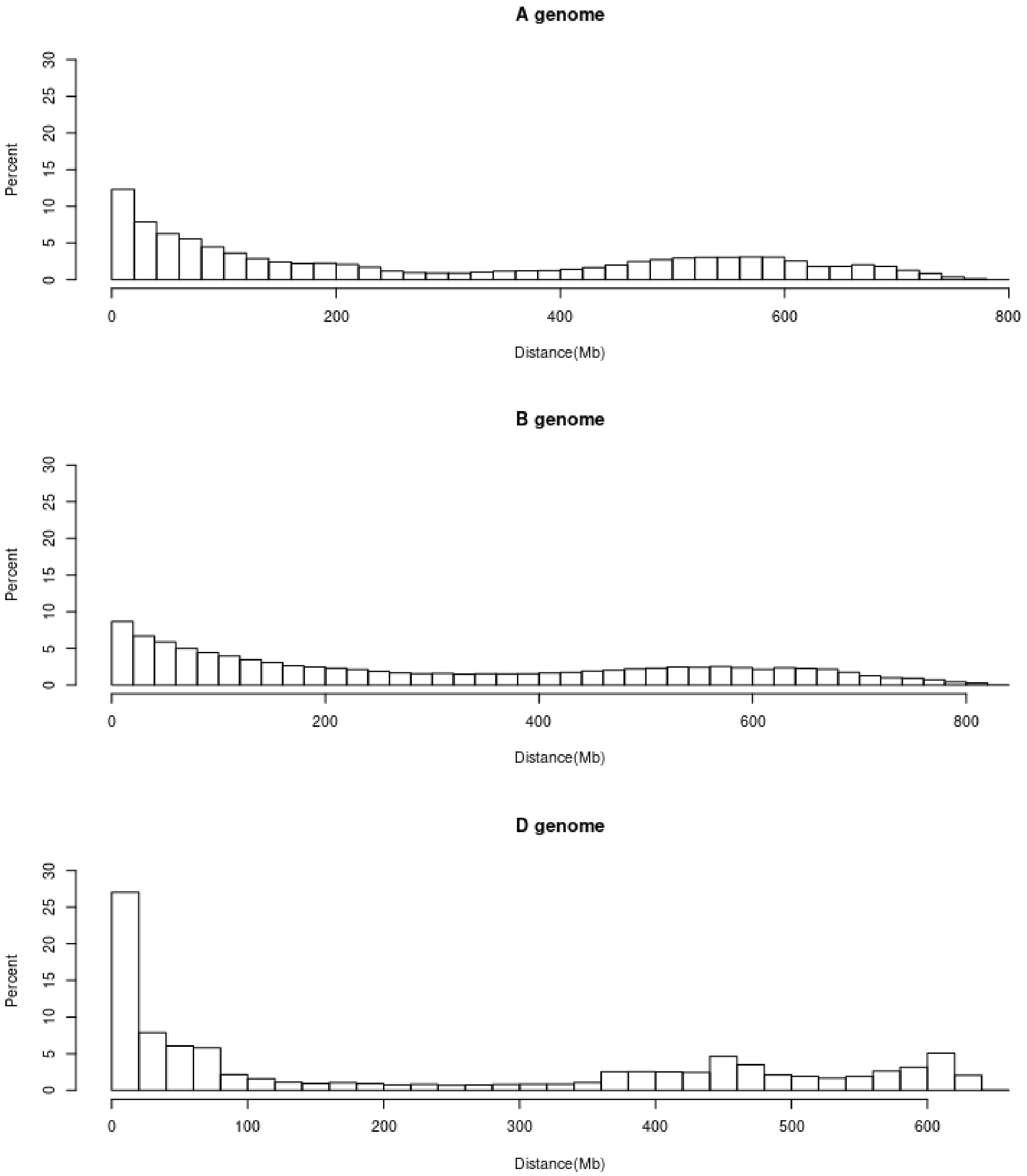

Figure S7. Percentual distribution of marker pairs in each of the three wheat genomes as a function of the physical distance (Mb)

Figure S8

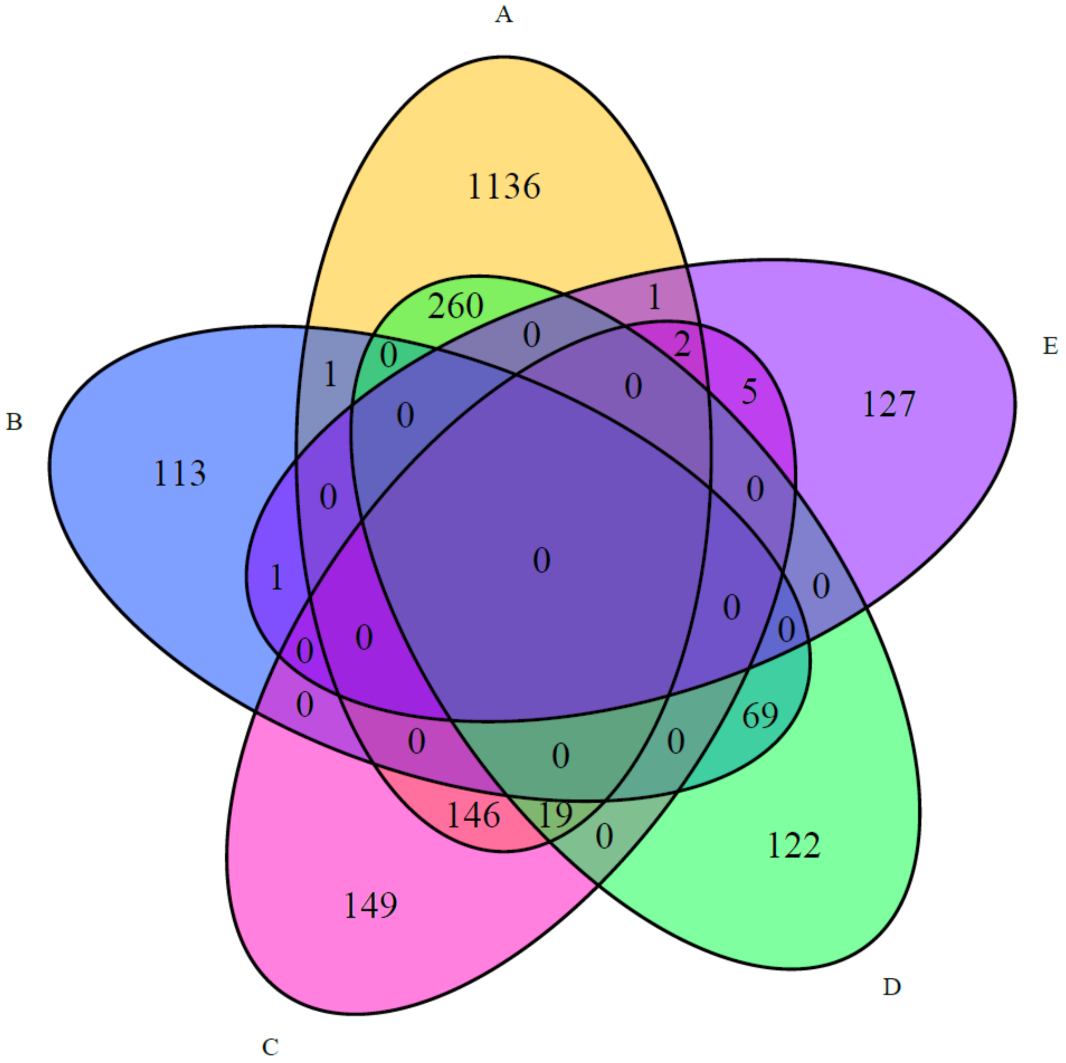

Figure S8. Venn diagram showing the amount of overlapping associations for leaf rust severity found by genome-wide exome association scans in a hybrid wheat population and its corresponding subpopulations.

The total hybrid wheat population is composed by 1,574 hybrids plus their 118 female and 15 male parent lines. Numbers correspond to the amount of overlapping single-nucleotide polymorphisms from exome capture sequencing having significant associations for leaf rust severity and detected in: the total population (A) and its subpopulations $\text{Top}_{25\%}$ (B), $\text{Inferior}_{75\%}$ (C), $\text{Top}_{50\%}$ (D) and $\text{Inferior}_{50\%}$ (E).

Figure S9

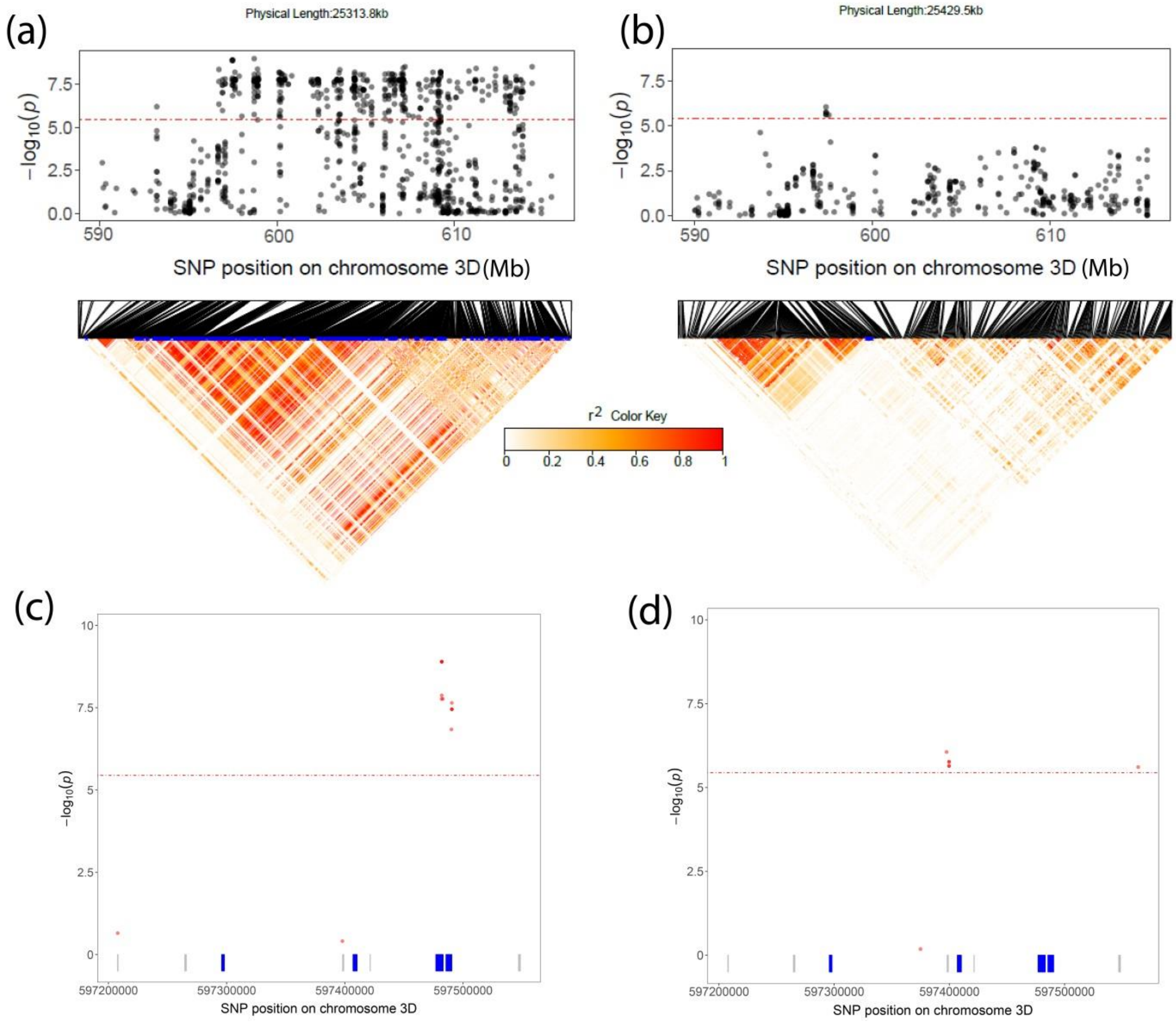

Figure S9. Extensive genomic region associated with leaf rust resistance on chromosome 3D detected by a genome-wide exome association scan for additive effects in a vast hybrid wheat population and narrowed down to a smaller candidate region using an independent validation population.

Manhattan plots showing the significant exome associations for additive effects underlying leaf rust detected within an extensive genomic region (590 – 615 Mb) on chromosome 3D in: (a) a vast hybrid wheat population of 1,574 hybrids plus their 118 female and 15 male parent lines and (b) a validation population of 128 hybrids plus their 24 female and 16 male parent lines. $-\log_{10}$(*P*-value)s of the significance test of additive effects are plotted against physical positions on chromosome 3D. Red horizontal dot-dashed lines indicate the multiple-test-corrected significance thresholds for association analysis. The upper-triangular halves of the linkage disequilibrium (LD, as r^2) matrices between single-nucleotide polymorphisms (SNPs) located within the extensive genomic region on chromosome 3D are shown as heatmaps directly below Manhattan plots. At the bottom, a close-up view of the candidate region (597.1 – 598.1 Mb) narrowed down by the independent-validation-population approach in the vast hybrid wheat and the independent validation population. Physical positions of SNPs belonging to genes with annotated resistance function and others SNPs are shown as vertical boxes in blue and gray, respectively.

Figure S10

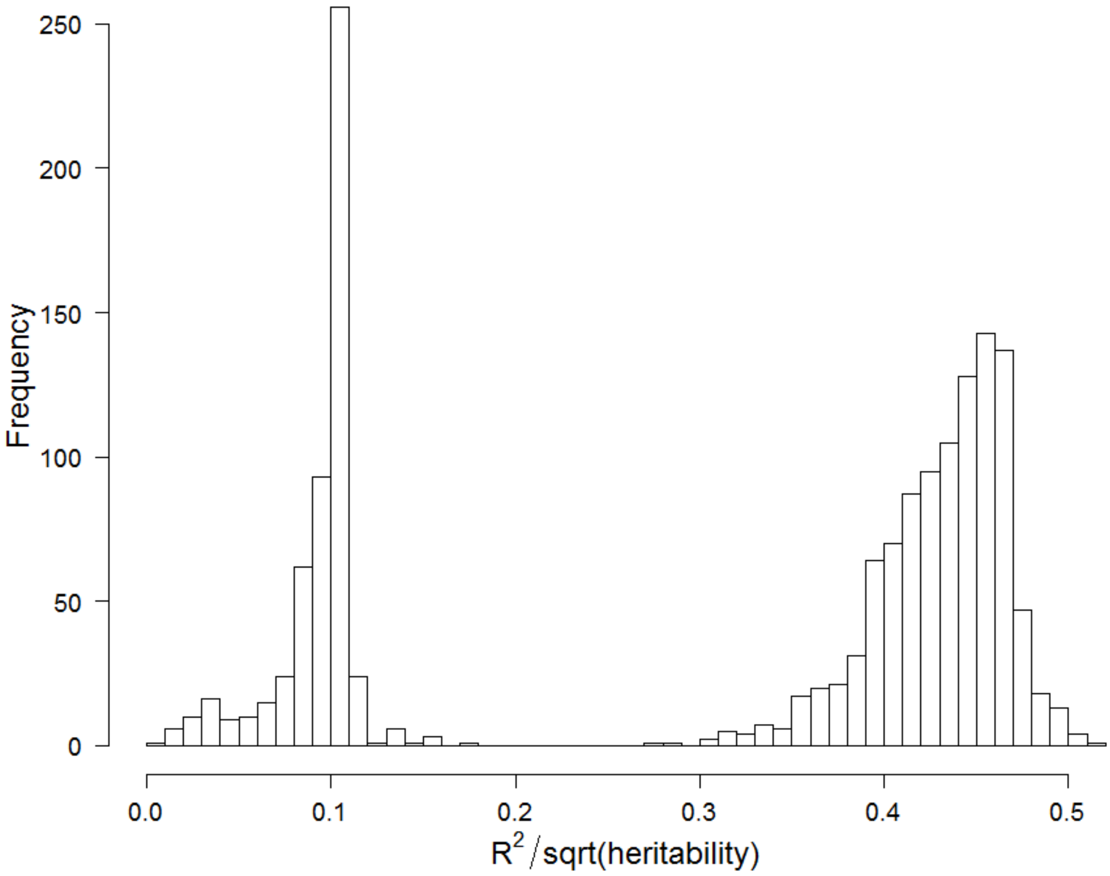

Figure S10. Histogram of the percentages of genetic variance (R^2/h) explained by single-nucleotide polymorphisms found as associated with leaf rust severity in a hybrid wheat population of 1,574 hybrids plus their 118 female and 15 male parent lines.

Figure S11

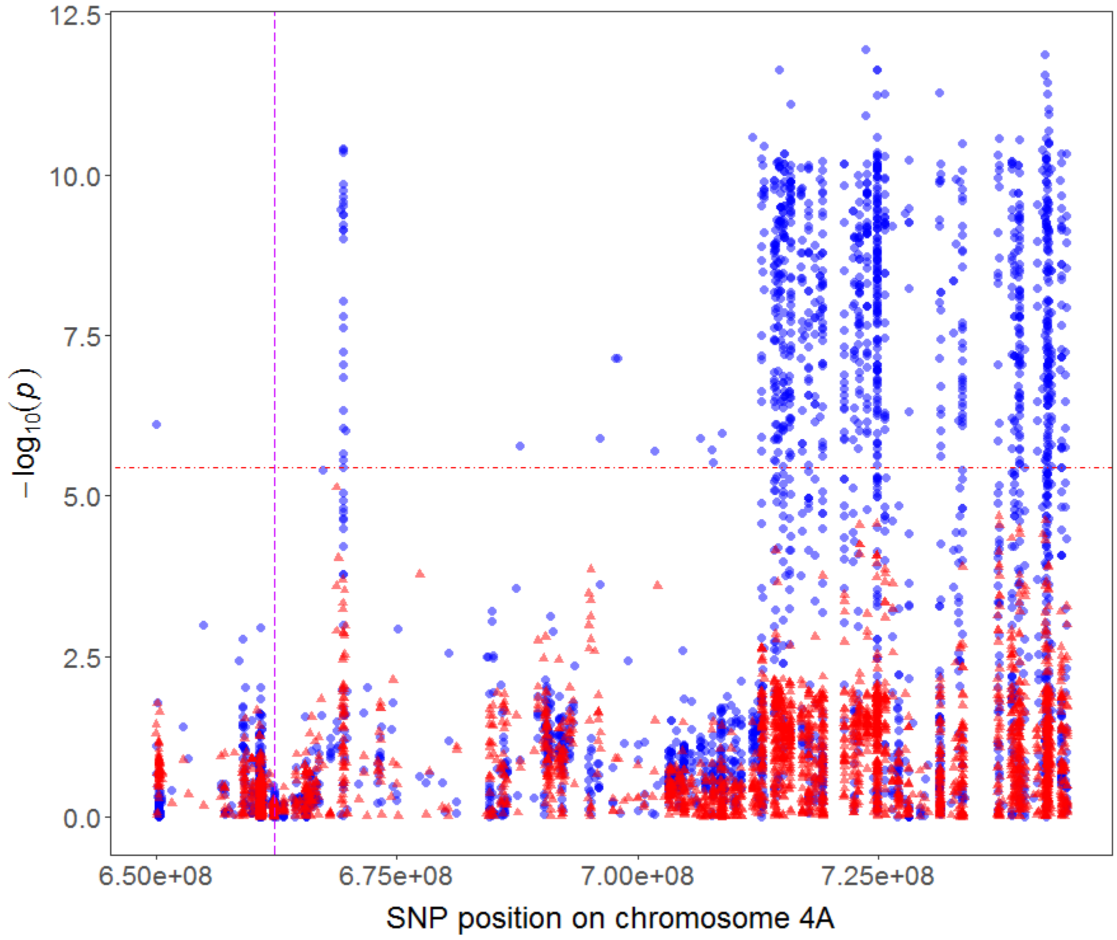

Figure S11. Close-up view of the two association peaks within a candidate region on chrosomosome 4A found by a genome-wide exome association scan for additive and dominance effects underlying leaf rust severity in a hybrid wheat population of 1,574 hybrids plus their 118 female and 15 male parents

The Manhattan plot shows the –$\log_{10}$(*P*-value)s of the significance test of additive (blue dots) and dominance (red triangles) effects underlying leaf rust severity as a function of physical positions (bp) on chromosomes. The black horizontal dot-dashed line indicates the genome-wide-multiple-test-corrected significance threshold for association analysis. The magenta vertical dashed line points out the position of the homologous gene of *Lr34.*

Figure S6

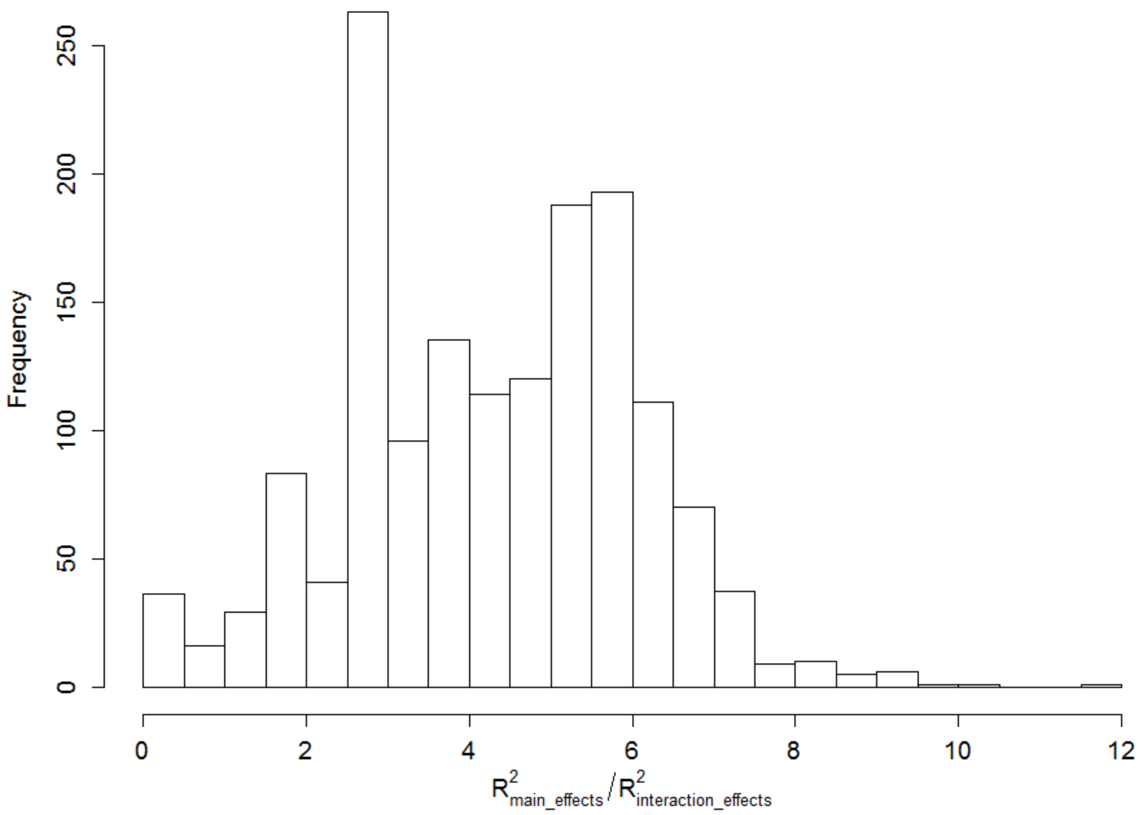

Figure S12. Histogram of the ratio of phenotypic variation explained by main additive and dominance effects ($\mathbf{R^2_{main\_effects}}$) over that explained by interaction effects with environments ($\mathbf{R^2_{interaction\_effects}}$) of single-nucleotide polymorphisms found as associated with leaf rust severity in a hybrid population (1,574 hybrids plus their 118 female and 15 male parent lines) tested in five environments.

Figure S7

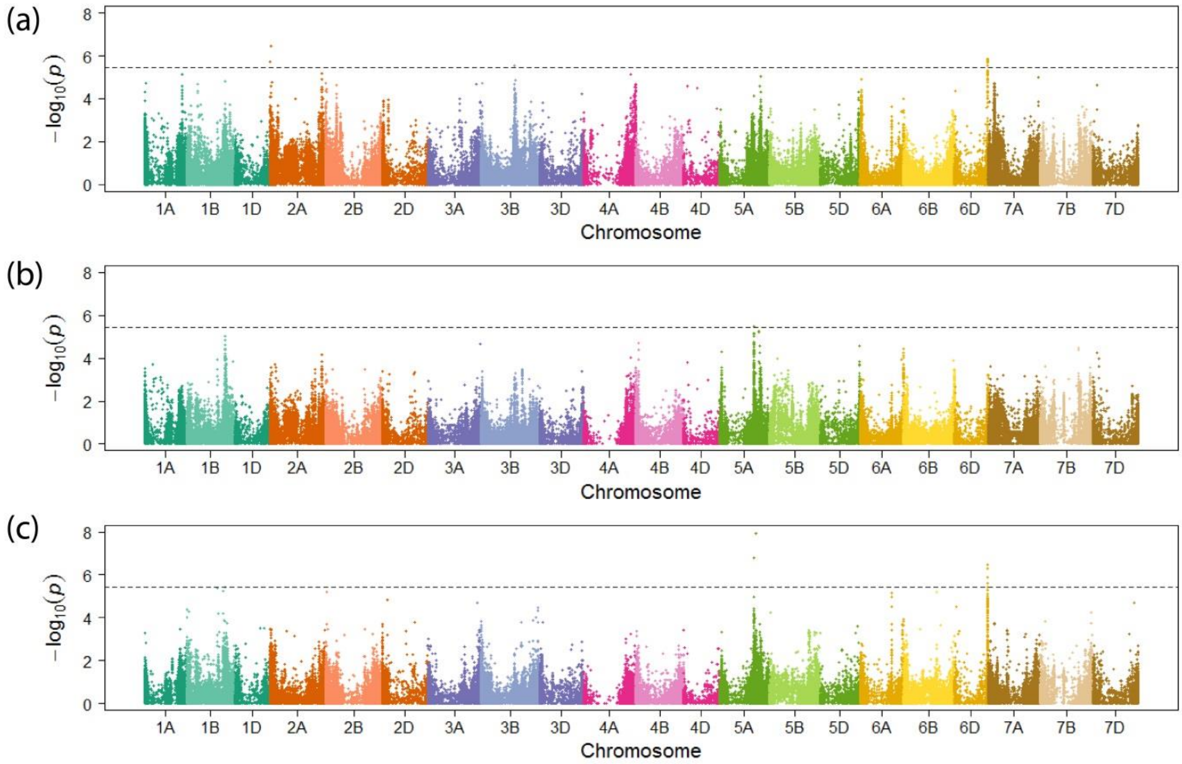

Figure S13. Genome-wide exome association scans for dominance effects underlying leaf rust severity in a vast hybrid wheat population and its different subpopulations.

Manhattan plots show the $-\log_{10}$(P-value)s of the significance test of dominance effects underlying leaf rust severity as a function of physical positions on chromosomes. The total hybrid wheat population is composed by 1,574 hybrids plus their 118 female and 15 male parent lines. Black horizontal dashed lines indicate the genome-wide-multiple-test-corrected significance threshold for association analysis. Genome-wide exome association scans for dominance effects were performed in: (a) total population and subpopulations (b) $\text{Top}_{25\%}$ and (c) $\text{Top}_{50\%}$.

Figure S8

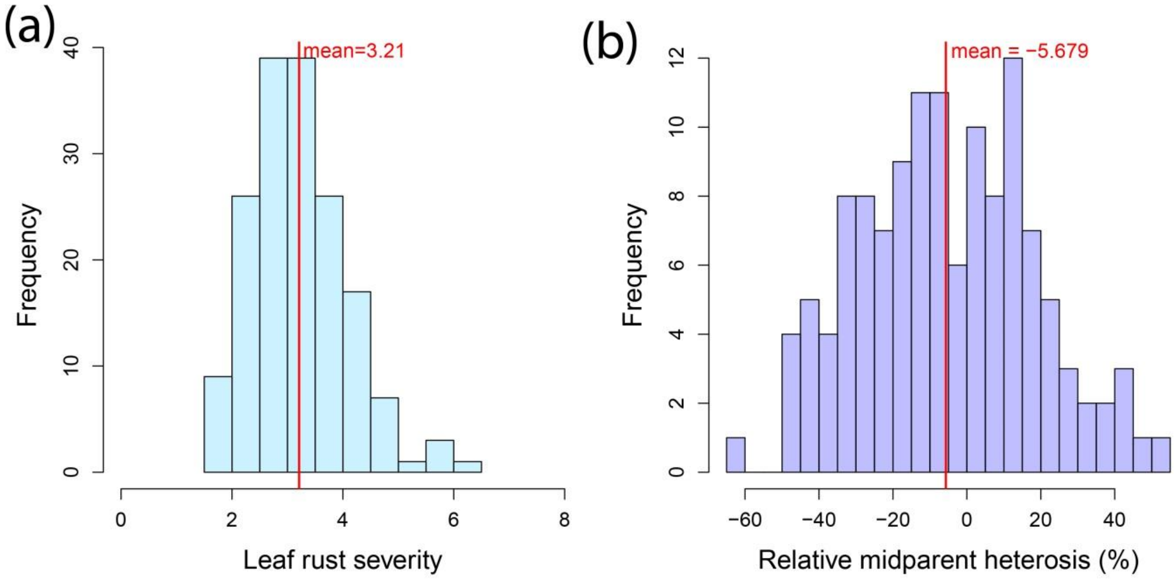

Figure S14. Distribution of leaf rust severity scores in the validation population.

(a) Histogram of leaf rust severity scores (1 = fully resistant, 9 = fully susceptible) of a hybrid population composed by 128 hybrids plus their 24 female and 16 male parents (b) Histogram of relative (%) midparent heterosis of 128 hybrids.

Figure S9

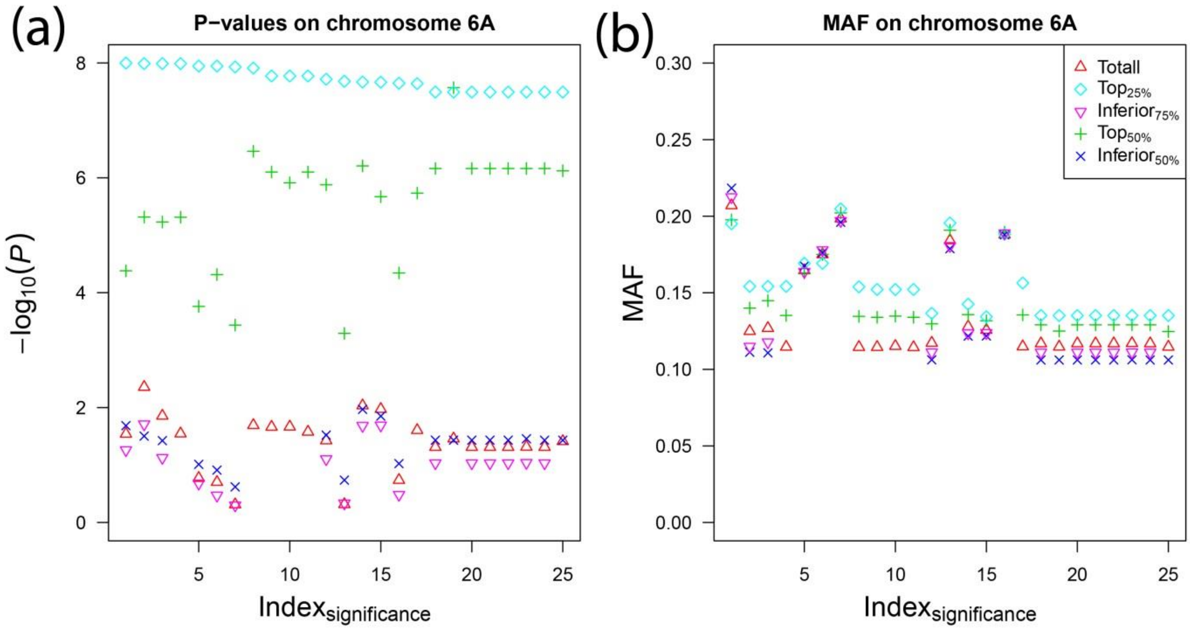

Figure S15. Some general statistics in a vast hybrid wheat population and its different subpopulations regarding associations mapping on chromosome 6A

(a) –$\log_{10}$(*P*-value)s of the significance test of additive effects for single nucleotide polymorphisms (SNPs) on chromosome 6A plotted against a significance index ($\text{Index}_{\text{Significance}}$) in the total population and its subpopulations $\text{Top}_{50\%}$, $\text{Inferior}_{50\%}$, $\text{Top}_{25\%}$ and $\text{Inferior}_{75\%}$. The $\text{Index}_{\text{Significance}}$ corresponds to the ranking position of decreasingly sorted -$\log_{10}$(*P-value*)s of SNPs with significant associations in the $\text{Top}_{25\%}$ subpopulation. (b) Minor allele frequency (MAF) plotted against the $\text{Index}_{\text{Significance}}$ in the total population and its subpopulations.

Figure S10

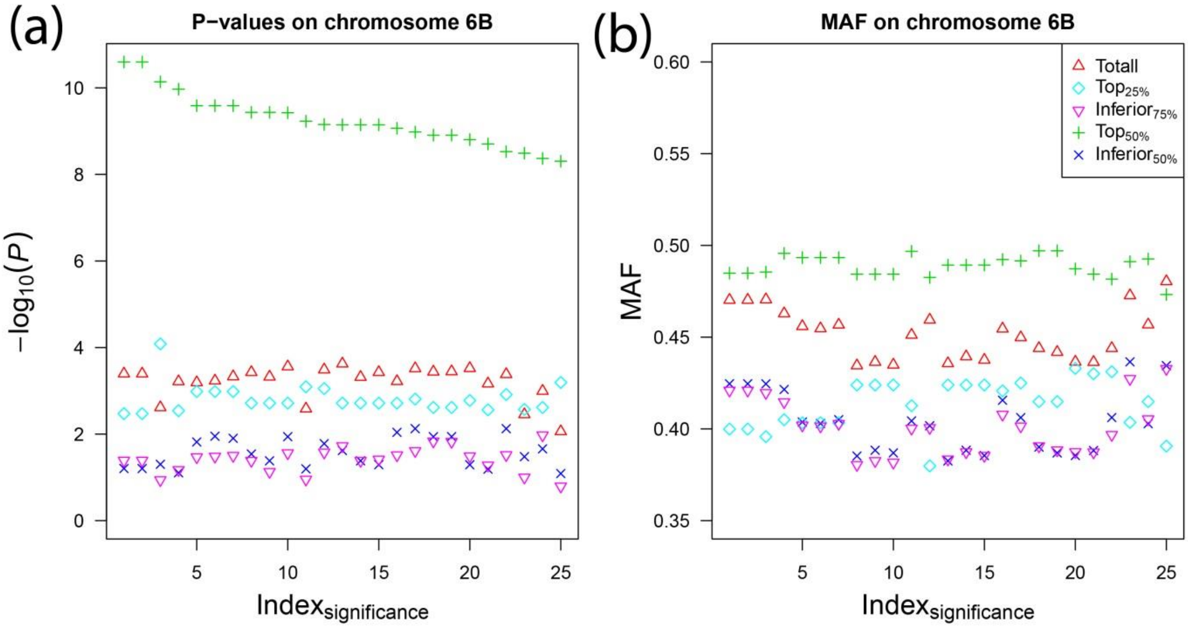

Figure S16. Some general statistics in a vast hybrid wheat population and its different subpopulations regarding associations mapping on chromosome 6B

(a) –log$_{10}$(*P*-value)s of the significance test of additive effects for single nucleotide polymorphisms (SNPs) on chromosome 6B plotted against a significance index (Index$_{Significance}$) in the total population and its subpopulations Top$_{50\%}$, Inferior$_{50\%}$, Top$_{25\%}$ and Inferior$_{75\%}$. The Index$_{Significance}$ corresponds to the ranking position of decreasingly sorted -log$_{10}$(*P-value*)s of SNPs with significant associations in the Top$_{50\%}$ subpopulation. (b) Minor allele frequency (MAF) plotted against the Index$_{Significance}$ in the total population and its subpopulations.

Figure S11

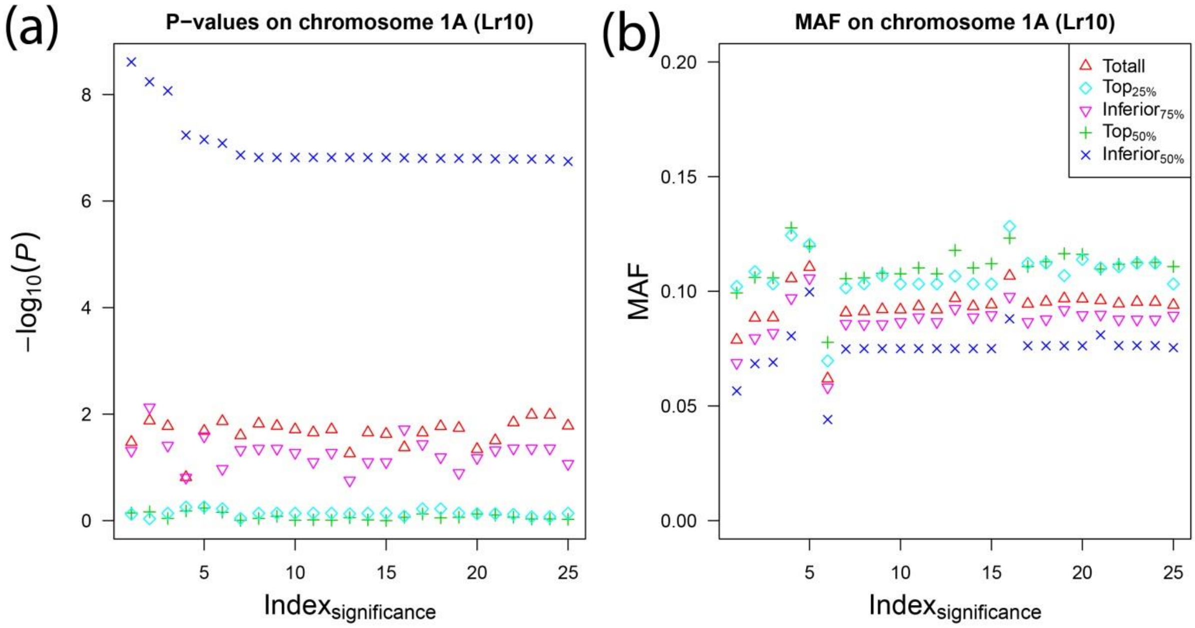

Figure S17. Some general statistics in a vast hybrid wheat population and its different subpopulations regarding associations mapping on chromosome 1A

(a) –log$_{10}$(*P*-value)s of the significance test of additive effects for single nucleotide polymorphisms (SNPs) on chromosome 1A plotted against a significance index (Index$_{\text{Significance}}$) in the total population and its subpopulations Top$_{50\%}$, Inferior$_{50\%}$, Top$_{25\%}$ and Inferior$_{75\%}$. The Index$_{\text{Significance}}$ corresponds to the ranking position of decreasingly sorted -log$_{10}$(*P-value*)s of SNPs with significant associations in the Inferior$_{50\%}$ subpopulation. (b) Minor allele frequency (MAF) plotted against the Index$_{\text{Significance}}$ in the total population and its subpopulations.

Figure S12

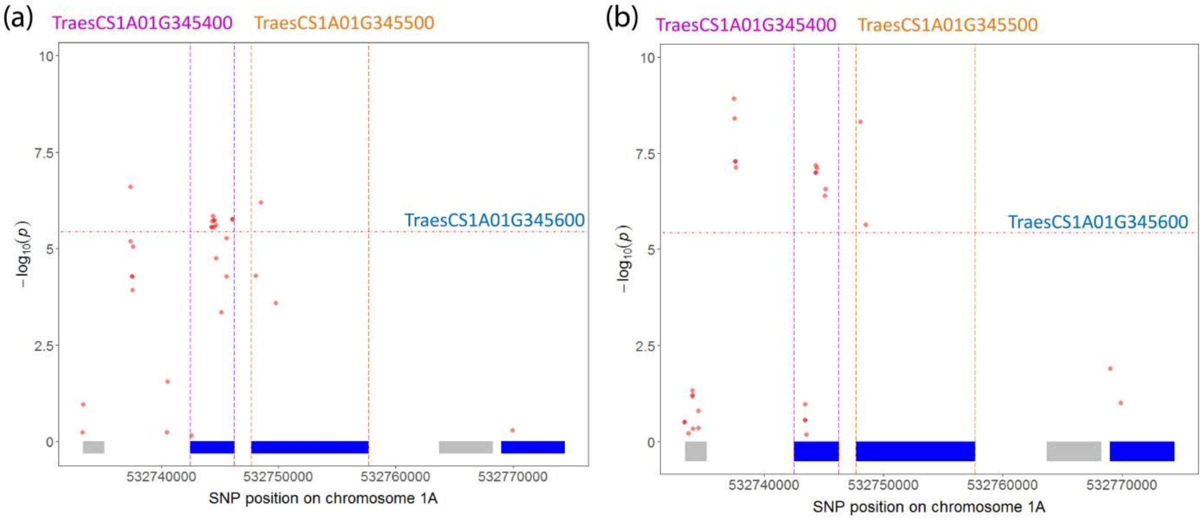

Figure S18. Candidate genes underlying significant associations on chromosome 1A

Manhattan plots showing candidate genes underlying significant associations for leaf rust additive effects on chromosome 1A found in: (a) a hybrid wheat population of 1,574 hybrids plus their 118 female and 15 male parent lines and (b) a validation population of 128 hybrids plus their 24 female and 16 male parent lines. $-\log_{10}$(*P*-value)s of the significance test of additive effects are plotted against physical positions on chromosome 1A. Red horizontal dot-dashed lines indicate the multiple-test-corrected significance thresholds for association analysis. The genes with annotated resistance function and others are shown as vertical boxes in blue and gray, respectively.

Table S1. Functional location and type of substitution (synonymous and non-synonymous) within the coding sequence for single-nucleotide polymorphisms (SNPs) present in a hybrid wheat population of 1,574 hybrids plus their 118 female and 15 male parent lines.

Functional location	SNPs			Percentage
Upstream gene (1Kb)	33,547			16.54
Five_prime_UTR	1,686			0.83
Coding sequence	41,634	Synonymous	19,468	20.52
		Non-synonymous	22,166	
Intron	28,299			13.95
Three_prime_UTR	7,616			3.75
Downstream gene (1kb)	31,905			15.73
Intergenic region	58,188			28.68

Table S2. Estimated average physical distance (Mb) according to different wheat chromosomes where the linkage disequilibrium (r^2) fell below r^2=0.2 in a hybrid wheat population of 1,574 hybrids plus their 118 female and 15 male parent lines

Chromosome	Distance (Mb)		
	A	B	D
1	3.18	11.26	19.56
2	6.43	12.5	3.85
3	4.16	8.57	6.48
4	14.19	5.62	4.28
5	6.14	6.37	2.43
6	2.93	8.5	1.16
7	6.98	2.2	8.69

Table S3. Expected impact of population stratification during genome-wide exome association scans for leaf rust severity on associations of single nucleotide polymorphisms (SNPs) mapping close to *Lr10* in a hybrid population of 1,574 hybrids plus their 118 female and 15 male parents and its subpopulations Top$_{25\%}$, Inferior$_{75\%}$, Top$_{50\%}$ and Inferior$_{50\%}$. The general impact of population structure was measured as the correlation between upper triangles of Roger's distance (RD) and absolute phenotypic distance (PD) matrices ($r_{RD,PD}$) while the specific impact on *Lr10* related associations was measured as the correlation between upper triangles of RD matrices using all SNPs and those RD portrayed by the corresponding associated SNPs pertaining *Lr10* ($r_{RD,Lr10}$).

Population	$r_{RD,PD}$	$r_{RD,Lr10}$
Total	0.082	0.092
Top$_{25\%}$	0.117	0.110
Inferior$_{75\%}$	0.072	0.096
Top$_{50\%}$	0.056	0.090
Inferior$_{50\%}$	0.068	0.098

Table S4. Estimates of variances components and heritabilities (h^2) for leaf rust severity in a hybrid wheat population composed by 1,574 hybrids produced by factorial crosses between 118 female (F) and 15 male (M) parents. Components correspond to genetic (σ_G^2), general (GCA, $\sigma_{GCA_F}^2$ and $\sigma_{GCA_M}^2$) and specific (SCA, σ_{SCA}^2) combining abilities variances, as well as those of the corresponding interactions with the environment ($\sigma_{G\times E}^2$, $\sigma_{GCA_{F\times E}}^2$ and $\sigma_{GCA_{M\times E}}^2$), excepting for the interaction between SCA and environment which is confounded with the error term in the σ_e^2 component.

Estimate	Leaf rust severity
Parents	
σ_G^2	1.343
$\sigma_{G\times E}^2$	0.567
h^2	0.81
Hybrids	

$\sigma^2_{GCA_F}$	1.247
$\sigma^2_{GCA_M}$	0.059
σ^2_{SCA}	0.081
$\sigma^2_{GCA_{F\times E}}$	0.484
$\sigma^2_{GCA_{M\times E}}$	0.027
σ^2_e	0.965
h^2	0.82

Table S5. Putative genes underlying significant regions on chromosome 4A.

Population	SNP	Chr	Position	P value of additve effect	P value of dominance effect	Gene	Type	Start position of gene	End position of gene
Top$_{50\%}$	S4_714567642	4A	714567642	2.25E-07	1.11E-01	TraesCS4A02G447900	CNL	714564380	714569033
Top$_{50\%}$	S4_714567666	4A	714567666	2.73E-07	2.27E-02	TraesCS4A02G447900	CNL	714564380	714569033
Top$_{50\%}$	S4_714567679	4A	714567679	3.22E-06	1.22E-01	TraesCS4A02G447900	CNL	714564380	714569033
Top$_{50\%}$	S4_715719194	4A	715719194	2.42E-06	9.21E-03	TraesCS4A02G449700	RLK	715713866	715719940
Top$_{50\%}$	S4_733422516	4A	733422516	2.88E-06	1.27E-02	TraesCS4A02G473300	RLK	733420749	733423532
Top$_{50\%}$	S4_733422628	4A	733422628	3.08E-06	7.25E-02	TraesCS4A02G473300	RLK	733420749	733423532
Top$_{50\%}$	S4_739606363	4A	739606363	2.48E-06	1.48E-02	TraesCS4A02G486500	CNL	739605514	739609783
Top$_{50\%}$	S4_739606393	4A	739606393	3.10E-06	1.15E-02	TraesCS4A02G486500	CNL	739605514	739609783
Top$_{50\%}$	S4_739606402	4A	739606402	1.34E-06	6.46E-02	TraesCS4A02G486500	CNL	739605514	739609783
Top$_{50\%}$	S4_739606752	4A	739606752	2.67E-07	2.93E-02	TraesCS4A02G486500	CNL	739605514	739609783
Top$_{50\%}$	S4_739607118	4A	739607118	3.59E-06	1.48E-01	TraesCS4A02G486500	CNL	739605514	739609783
Inferior$_{75\%}$	S4_714567666	4A	714567666	1.86E-06	1.43E-02	TraesCS4A02G447900	CNL	714564380	714569033
Inferior$_{75\%}$	S4_714567716	4A	714567716	1.61E-06	2.78E-02	TraesCS4A02G447900	CNL	714564380	714569033
Inferior$_{75\%}$	S4_715008817	4A	715008817	8.92E-07	6.44E-02	TraesCS4A02G448600	CNL	715006340	715010565
Inferior$_{75\%}$	S4_715008948	4A	715008948	9.57E-07	8.08E-02	TraesCS4A02G448600	CNL	715006340	715010565
Inferior$_{75\%}$	S4_715008955	4A	715008955	9.57E-07	8.08E-02	TraesCS4A02G448600	CNL	715006340	715010565
Inferior$_{75\%}$	S4_715008965	4A	715008965	8.86E-07	2.83E-01	TraesCS4A02G448600	CNL	715006340	715010565
Inferior$_{75\%}$	S4_715719211	4A	715719211	2.43E-07	7.36E-02	TraesCS4A02G449700	RLK	715713866	715719940
Inferior$_{75\%}$	S4_739606340	4A	739606340	6.62E-07	2.99E-01	TraesCS4A02G486500	CNL	739605514	739609783
Inferior$_{75\%}$	S4_739608379	4A	739608379	1.39E-06	2.69E-01	TraesCS4A02G486500	CNL	739605514	739609783
Inferior$_{75\%}$	S4_739608609	4A	739608609	4.75E-07	2.34E-01	TraesCS4A02G486500	CNL	739605514	739609783
Total	S4_644002378	4A	644002378	1.47E-06	2.81E-01	TraesCS4A02G371100	RLK	643998553	644002766
Total	S4_714567069	4A	714567069	1.69E-08	8.80E-03	TraesCS4A02G447900	CNL	714564380	714569033
Total	S4_714567642	4A	714567642	6.45E-09	2.85E-02	TraesCS4A02G447900	CNL	714564380	714569033
Total	S4_714567666	4A	714567666	3.88E-09	1.98E-02	TraesCS4A02G447900	CNL	714564380	714569033
Total	S4_714567672	4A	714567672	2.11E-06	5.96E-02	TraesCS4A02G447900	CNL	714564380	714569033
Total	S4_714567679	4A	714567679	1.32E-06	4.14E-02	TraesCS4A02G447900	CNL	714564380	714569033
Total	S4_714567680	4A	714567680	6.94E-09	3.47E-02	TraesCS4A02G447900	CNL	714564380	714569033
Total	S4_714567716	4A	714567716	2.31E-09	2.51E-02	TraesCS4A02G447900	CNL	714564380	714569033
Total	S4_714523255	4A	714523255	9.92E-10	1.89E-02	TraesCS4A02G447700	CN	714520133	714523356
Total	S4_714523329	4A	714523329	4.80E-09	2.77E-02	TraesCS4A02G447700	CN	714520133	714523356
Total	S4_715006830	4A	715006830	9.69E-07	9.20E-01	TraesCS4A02G448600	CNL	715006340	715010565
Total	S4_715008802	4A	715008802	3.38E-06	3.47E-02	TraesCS4A02G448600	CNL	715006340	715010565
Total	S4_715008807	4A	715008807	4.15E-07	1.79E-02	TraesCS4A02G448600	CNL	715006340	715010565
Total	S4_715008809	4A	715008809	8.24E-07	4.73E-02	TraesCS4A02G448600	CNL	715006340	715010565
Total	S4_715008817	4A	715008817	5.15E-08	1.80E-02	TraesCS4A02G448600	CNL	715006340	715010565
Total	S4_715008884	4A	715008884	4.89E-10	5.00E-02	TraesCS4A02G448600	CNL	715006340	715010565
Total	S4_715008892	4A	715008892	8.40E-10	3.93E-01	TraesCS4A02G448600	CNL	715006340	715010565
Total	S4_715008893	4A	715008893	8.40E-10	3.93E-01	TraesCS4A02G448600	CNL	715006340	715010565
Total	S4_715008895	4A	715008895	3.86E-10	4.14E-02	TraesCS4A02G448600	CNL	715006340	715010565
Total	S4_715008948	4A	715008948	5.97E-10	8.66E-02	TraesCS4A02G448600	CNL	715006340	715010565
Total	S4_715008955	4A	715008955	3.81E-10	7.68E-02	TraesCS4A02G448600	CNL	715006340	715010565
Total	S4_715008965	4A	715008965	4.58E-08	1.20E-01	TraesCS4A02G448600	CNL	715006340	715010565
Total	S4_715719099	4A	715719099	7.06E-07	7.98E-02	TraesCS4A02G449700	RLK	715713866	715719940
Total	S4_715719102	4A	715719102	3.18E-10	2.61E-02	TraesCS4A02G449700	RLK	715713866	715719940
Total	S4_715719108	4A	715719108	2.29E-10	4.17E-02	TraesCS4A02G449700	RLK	715713866	715719940
Total	S4_715719188	4A	715719188	1.39E-10	5.56E-02	TraesCS4A02G449700	RLK	715713866	715719940
Total	S4_715719194	4A	715719194	8.45E-11	3.96E-02	TraesCS4A02G449700	RLK	715713866	715719940
Total	S4_715719204	4A	715719204	2.99E-07	1.12E-01	TraesCS4A02G449700	RLK	715713866	715719940
Total	S4_715719211	4A	715719211	1.63E-10	5.58E-02	TraesCS4A02G449700	RLK	715713866	715719940
Total	S4_715719646	4A	715719646	3.63E-07	1.91E-01	TraesCS4A02G449700	RLK	715713866	715719940
Total	S4_722298718	4A	722298718	1.29E-06	6.87E-02	TraesCS4A02G457000	RLK	722297019	722299894
Total	S4_722299775	4A	722299775	1.09E-08	3.83E-02	TraesCS4A02G457000	RLK	722297019	722299894

Total	S4_722299824	4A	722299824	1.95E-09	4.91E-02	TraesCS4A02G457000	RLK	722297019	722299894
Total	S4_722293596	4A	722293596	3.70E-10	1.21E-02	TraesCS4A02G456900	RLK	722287491	722294625
Total	S4_733422516	4A	733422516	1.27E-10	4.70E-02	TraesCS4A02G473300	RLK	733420749	733423532
Total	S4_739628932	4A	739628932	1.25E-07	1.85E-01	TraesCS4A02G486600	NL	739627540	739630396
Total	S4_739605754	4A	739605754	2.46E-09	2.69E-01	TraesCS4A02G486500	CNL	739605514	739609783
Total	S4_739605799	4A	739605799	3.18E-09	1.60E-01	TraesCS4A02G486500	CNL	739605514	739609783
Total	S4_739605920	4A	739605920	9.17E-08	7.78E-01	TraesCS4A02G486500	CNL	739605514	739609783
Total	S4_739606019	4A	739606019	6.66E-08	2.50E-01	TraesCS4A02G486500	CNL	739605514	739609783
Total	S4_739606027	4A	739606027	1.28E-08	9.02E-02	TraesCS4A02G486500	CNL	739605514	739609783
Total	S4_739606050	4A	739606050	2.95E-08	1.72E-02	TraesCS4A02G486500	CNL	739605514	739609783
Total	S4_739606293	4A	739606293	3.18E-06	8.97E-02	TraesCS4A02G486500	CNL	739605514	739609783
Total	S4_739606340	4A	739606340	1.62E-08	2.18E-01	TraesCS4A02G486500	CNL	739605514	739609783
Total	S4_739606363	4A	739606363	4.64E-10	3.34E-02	TraesCS4A02G486500	CNL	739605514	739609783
Total	S4_739606393	4A	739606393	2.82E-10	2.46E-02	TraesCS4A02G486500	CNL	739605514	739609783
Total	S4_739606444	4A	739606444	1.59E-08	2.09E-02	TraesCS4A02G486500	CNL	739605514	739609783
Total	S4_739606514	4A	739606514	5.03E-08	5.31E-01	TraesCS4A02G486500	CNL	739605514	739609783
Total	S4_739606726	4A	739606726	5.26E-10	1.67E-02	TraesCS4A02G486500	CNL	739605514	739609783
Total	S4_739606752	4A	739606752	9.13E-11	3.45E-02	TraesCS4A02G486500	CNL	739605514	739609783
Total	S4_739607084	4A	739607084	4.32E-07	5.67E-02	TraesCS4A02G486500	CNL	739605514	739609783
Total	S4_739607118	4A	739607118	2.54E-07	1.30E-01	TraesCS4A02G486500	CNL	739605514	739609783
Total	S4_739607272	4A	739607272	2.76E-06	3.82E-03	TraesCS4A02G486500	CNL	739605514	739609783
Total	S4_739607459	4A	739607459	1.02E-09	1.09E-01	TraesCS4A02G486500	CNL	739605514	739609783
Total	S4_739608064	4A	739608064	2.51E-08	1.13E-02	TraesCS4A02G486500	CNL	739605514	739609783
Total	S4_739608099	4A	739608099	3.27E-10	2.87E-02	TraesCS4A02G486500	CNL	739605514	739609783
Total	S4_739608132	4A	739608132	6.45E-09	1.58E-01	TraesCS4A02G486500	CNL	739605514	739609783
Total	S4_739608151	4A	739608151	2.49E-07	1.05E-01	TraesCS4A02G486500	CNL	739605514	739609783
Total	S4_739608185	4A	739608185	1.23E-06	8.00E-03	TraesCS4A02G486500	CNL	739605514	739609783
Total	S4_739608251	4A	739608251	4.37E-08	1.77E-02	TraesCS4A02G486500	CNL	739605514	739609783
Total	S4_739608371	4A	739608371	1.08E-08	1.13E-02	TraesCS4A02G486500	CNL	739605514	739609783
Total	S4_739608379	4A	739608379	1.65E-08	3.98E-02	TraesCS4A02G486500	CNL	739605514	739609783
Total	S4_739608609	4A	739608609	7.60E-09	1.77E-01	TraesCS4A02G486500	CNL	739605514	739609783
Total	S4_739608735	4A	739608735	4.82E-10	3.08E-02	TraesCS4A02G486500	CNL	739605514	739609783
Total	S4_739866815	4A	739866815	8.91E-08	2.39E-02	TraesCS4A02G487600	NBS	739860752	739867409
Total	S4_742035108	4A	742035108	3.85E-10	2.19E-02	TraesCS4A02G493600	NL	742032665	742036031
Total	S4_742035163	4A	742035163	8.25E-11	3.79E-02	TraesCS4A02G493600	NL	742032665	742036031